Clays and Clay Minerals, Vol. 23, pp. 369–375. Pergamon Press 1975. Printed in Great Britain

THE SYNTHESES OF HYDROTALCITE-LIKE COMPOUNDS AND THEIR STRUCTURES AND PHYSICO-CHEMICAL PROPERTIES—I: THE SYSTEMS Mg^{2+}–Al^{3+}–NO_3^-, Mg^{2+}–Al^{3+}–Cl^-, Mg^{2+}–Al^{3+}–ClO_4^-, Ni^{2+}–Al^{3+}–Cl^- AND Zn^{2+}–Al^{3+}–Cl^-

SHIGEO MIYATA

Kyowa Chemical Industry Co. Ltd., Yashimanishi-machi, Takamatsu-shi, Japan

(*First received* 24 *September* 1974; *and in final form* 24 *May* 1975)

Abstract—The basic salts of this system were prepared and their structures and physico-chemical properties were studies by electron microscopy, chemical analysis, X-ray powder diffraction, thermal analysis, i.r. absorption spectra, BET absorption, and acidity–basicity measurements. The salts were found to be new compounds analogous to hydrotalcite. They can be expressed by the formula; $[M_x^{2+}M_y^{3+}(OH)_{2(x+y)}]^{y+}\ [A_{z_1}^-A_{z_2}^{2-}\cdot mH_2O]^{-(z_1+2z_2)}$ where M^{2+} and M^{3+} denote di- and trivalent cations, A^- and A^{2-} denote mono- and divalent anions, respectively, and $y = z_1 + 2z_2$; $z_1 \gg z_2$.

The structures consist of positively charged $Cd(OH)_2$-like basic layers and intermediate layers formed from anions and water molecules with the solid solution of divalent cation (M^{2+}) and trivalent cation (M^{3+}) being formed in the range of $0.6 < x/(x + y) < 0.9$. The anions of Cl^-, NO_3^- and ClO_4^- are easily substituted by CO_3^{2-}. A large part of the NO_3^- makes a monodentate-type bond and the ClO_4^- a bridge-type bond.

INTRODUCTION

A series of hydrotalcite-like compounds, which are expressed by the following general formula, was reported previously (Brown and Gastuche, 1967, Allmann, 1970, Miyata and Kumura, 1973): $M_x^{2+}M_y^{3+}(OH)_{2x+3y-nz}(A^{n-})_z\cdot mH_2O$, where M^{2+} and M^{3+} are divalent and trivalent cations, respectively, and A^{n-} are n valent anions.

Since the synthesized hydrotalcites are utilized as acid adsorbents and catalyst carriers in industry, the hydrotalcite-like compounds also are expected to be similarly utilized. This detailed study may promise new application of the compounds as a gas adsorbent or as a catalyst.

In the present paper, the syntheses of the compounds containing various monovalent inorganic anions and their structrues and physico-chemical properties are reported.

EXPERIMENTAL

Preparation of compounds

Samples A,B,C,D and E were prepared as follows. About 200 ml of decarbonated and deionized water was put into a 1 liter four neck round flask filled by nitrogen gas and stirred at about 25°C with a magnetic stirrer. The mixture (Al^{3+} = 0.25 mol/l, Mg^{2+} = 0.75 mol/l) of decarbonated aluminum chloride (B,C,D,E,F) or nitrate (A,H), magnesium chloride (B,C,D,E,F) or nitrate (A,H) solution and aqueous solution (2 mol/l) of sodium hydroxide were added dropwise from a burette, the pH of the reaction mixture being kept at about 10. The precipitate obtained was filtered, washed with water and dried at 70°C for 15 hr. In the preparation of sample F, ammonia gas was used instead of sodium hydroxide, the other procedure being the same as above.

Samples of G,H,I,J and K were prepared by a different procedure. About 500 ml of water was put into a 2.5 liter stainless steel reaction vessel and kept at 25°C by operating a chemi-stirrer. Then, the mixture (Al^{3+} = 0.25 mol/l, Mg^{2+} = 0.75 mol/l) of aluminum chloride (I,J,K), nitrate (H) or perchlorate (G), magnesium chloride (I,J,K), nitrate (H) or perchlorate (G) and aqueous solution (2 mol/l) of sodium hydrocide were added continuously at the total supply rate of about 80 ml/min by using a feeder, the pH of the reaction mixture being maintained at 10.0–10.2 during the reaction. The precipitate treatment was the same as above. All water was decarbonated and deionized before use.

Electron microscopy

Electron micrographs of the samples suspended in ethanol and dispersed supersonically for 5 min were taken by the transmission method with a Nihon Denshi JEM-T7S type electron microscope. Accelerating voltage was 60 kV and magnification 20000×.

Chemical analysis

The amount of Al, Mg, Ni, and Zn were determined by the chelate titrations of the samples dissolved in dilute hydrochloric acid. The Cl^- and ClO_4^- was determined by back-titrating the sample solution with

C.C.M. 23/5—C

Table 1. Chemical analysis and atomic ratio

Sample No.	Wt %						Atomic ratio		
	Al_2O_3	$M^{2+}O$	CO_2	A^-	Ig loss	Water content*	†	‡	§
A;Mg–Al–NO_3	15.4	34.9	0.87	15.5	48.9	7.99	2.87	0.830	0.960
B;Mg–Al–Cl	30.7	26.8	2.05	8.12	41.5	8.54	1.11	0.380	0.535
C;Mg–Al–Cl	20.3	32.8	1.30	11.3	46.3	10.3	2.05	0.805	0.955
D;Mg–Al–Cl	17.2	37.6	0.46	11.4	43.9	7.00	2.78	0.954	0.964
E;Mg–Al–Cl	13.7	41.8	0.73	9.20	44.3	6.92	3.86	0.965	1.09
F;Mg–Al–Cl	16.5	39.7	1.07	10.4	43.8	6.27	3.00	0.905	1.06
G;Mg–Al–ClO_4	13.9	33.5	0.89	19.8	51.4	6.12	3.06	0.730	0.880
H;Mg–Al–NO_3	15.9	37.6	1.26	16.4	45.6	6.09	2.99	0.848	1.03
I;Mg–Al–Cl	17.3	39.2	1.95	9.23	44.1	5.93	2.86	0.765	1.03
J;Ni–Al–Cl	12.2	51.2	1.20	7.30	36.0	8.04	2.88	0.865	1.10
K;Zn–Al–Cl	11.3	54.9	0.92	9.40	34.1	6.14	3.04	1.20	1.39

* Weight loss during heating at 105°C for 3 hr
† M^{2+}/M^{3+}
‡ A^-/M^{3+}
§ $(A^- + 2CO_3^{2-})/M^{3+}$ (total anion).

a 0.1 mol/l solution of ammonium thiocyanate with ammonium ferric sulfate as an indicator. The sample solution was made by dissolving the sample into nitrous acid, adding an excess of silver nitrate and diluted nitric acid while warming the solution. The amount of NO_3^- was measured by reducing NO_3^- of the sample with a mixture of a sodium hydroxide solution and Debalda alloy to form NH_3 and back-titrating the excess of sulfuric acid, which absorbed NH_3, with an aqueous sodium hydroxide. The amount of CO_3^{2-} was determined by a AGK carbonate salt measurement method.

X-ray powder diffraction, i.r. absorption and thermal analysis

The powder pattern of each sample was obtained with a Phillips X-ray diffractometer using filtered Cu-K_α radiation. The i.r. absorption spectra of the sample in the form of a KBr tablet were recorded for 400–4000 cm^{-1} with an Hitachi EPI-G3 i.r. spectrophotometer. The DTA and TGA diagrams were recorded for 200–350 mg samples with a Rigaku Denki DG-CIH unit at a heating-rate of 5°C/min.

Surface area and surface acidity–basicity

Surface area were measured by the BET method with nitrogen gas. The samples dried at 70°C were evacuated at room temperature for 1 hr. Other samples were calcined in air at 200°C for 1 hr and then evacuated at 150°C for 1 hr before measurement.

Acidity and basicity were measured by titration with *n*-butylamine and benzoic acid using a series of Hammett and nitroaniline indicators as previously reported (Miyata *et al.*, 1971).

Table 2. Relation between atomic ratio $(M^{3+}/(M^{2+} + M^{3+}))$ and total anion $((A^- + 2CO_3^{2-})/(M^{2+} + M^{3+}))$

Sample No.	B	C	D	E
$(Cl^- + 2CO_3^{2-})/(M^{2+} + M^{3+})$	0.213	0.314	0.278	0.216
$M^{3+}/(M^{2+} + M^{3+})$	0.474	0.340	0.265	0.205

RESULTS AND DISCUSSION

Electron micrographs

The samples are poorly dispersed, thin leaf-like aggregates analogous to synthesized hydrotalcite.

Chemical analysis

The results of chemical analysis are shown in Table 1. The ratio, $(A^- + 2CO_3^{2-})/M^{3+}$, of the total anions to aluminum ions at $M^{2+}/M^{3+} = 3$, is almost unity except for samples J and K. The value is in agreement with that of synthesized hydrotalcite (Miyata *et al.*, 1971). The larger values of samples J and K are considered to be due to the mixing of a small amount of carbonate because the logarithmic values of the solubility products of $NiCO_3$ and $ZnCO_3$ are less than half that of $MgCO_3$. The percentage of monovalent anion for total anions was about 90% under the flow of nitrogen gas and about 70% when exposed to air. Therefore, the monovalent anion is considered to be the main anion and to occupy the same lattice point as that of carbonate ion. It is also thought that the reactivity of the carbonate ion is stronger than that of the monovalent anion.

In the Mg^{2+}–Al^{3+}–Cl^- system the anion content increases with the increase of the aluminum ion content except for sample B. The ratio of $(A^- + 2CO_3^{2-})/M^{3+}$ should be unity if one assumes that the positively charged compound, $[Mg_{1-x}Al_x(OH_2)]^{x+}$, is formed by substituting the aluminum ion for the magnesium ion of the brucite-like layer. The anion existing between the layers has the charge of $-x$ in order to maintain electrical neutrality. As shown in Table 2, the observed values verify the validity of this assumption. The deviation observed for sample B is probably due to the fact that the ratio of Mg^{2+}/Al^{3+} exceeds the limit of substitution of Mg^{2+} by Al^{3+} (the limit

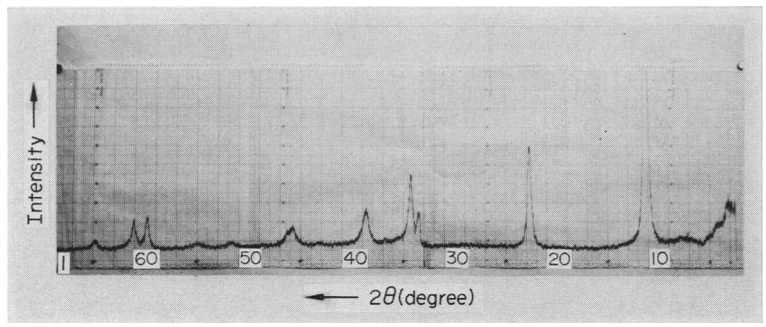

Fig. 1. X-ray powder diffraction for sample F.

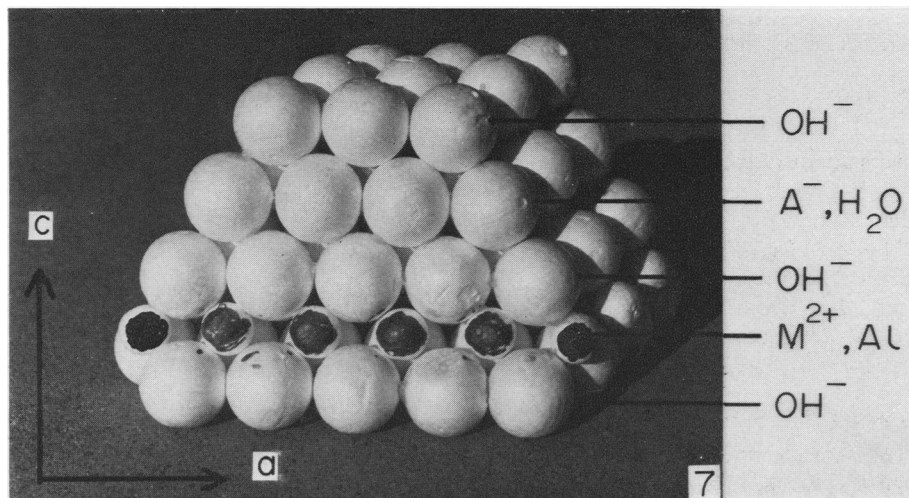

Fig. 7. Structural model of new hydrotalcite-like compounds.

https://doi.org/10.1346/CCMN.1975.0230508 Published online by Cambridge University Press

Table 3. Indexing of powder pattern of the compound in the sample F with $a_0 = 3.07$, $c_0 = 23.90$ or 15.93 Å

1 d obs.	2 d calc.	3 hkl	4 hkl
20.5 Å	23.9 Å	001	
11.5	11.9	002	
7.97	7.97	003	002
3.976	3.983	006	004
2.650	2.656	100, 009	100, 006
	2.619		101
2.609	2.592	102	
2.292	2.321	105	
2.021	1.991	00, 12	008
1.988	1.985	108	
1.533	1.533	110	110
	1.530	111	
1.505	1.505	113	112
1.431	1.431	116	114
1.317	1.319	202	
1.277	1.279	205	

1—Observed reflections.
2—Calculated spacings for hexagonal cells with $a = 3.07$, $c = 23.90$ and 15.93 Å.
3 and 4—Indices for reflections from cells with $a = 3.07$ and $c = 23.90$ and 15.93 Å, respectively.

is $Mg^{2+}/Al^{3+} = 1.5$ for synthesized hydrotalcite). This is explained by the fact that bayerite forms as a byproduct according to X-ray diffraction analysis.

X-ray powder diffraction

According to observations with X-ray diffraction and optical microscopy every sample consists of spherical aggregates (about 10–50 μm) which are formed by strong coagulation of microcrystallites (order of magnitude: 100 Å). The powder pattern observed for sample F (Mg^{2+}–Al^{3+}–Cl^-) is shown in Fig. 1. The other samples showed the analogous patterns to that shown in Fig. 1. The pattern for every sample, which consists of sharp and symmetrical peaks and some asymmetrical peaks at high angle of 30°2θ, is characteristic of clay minerals having a layer structure and very similar to the pattern of hydrotalcite. In order to verify this, the indexing was done as follows. Because the highest peak of $d \doteqdot 8$ Å corresponds to the pile of three oxygen sheets and is considered to be a unit layer, the cell dimension C_o was assumed to be an intergral multiple of the layer thickness. The cell dimension a_o should be almost the same as that of brucite, $d = 1.55$ Å was assumed to be (110). The indexing was done by assuming a hexagonal cell of the cell dimensions $a_o \doteqdot 3.10$ Å and $c_o \doteqdot n \times 8$ Å (n = integer). The result is shown in Tables 3 and 4. When n is 2, all the reflections can be fairly well interpreted, but the reflection corresponding to (001) is not observed and the indexing of the weak reflections of $d = 11.5$ Å and 20.5 Å cannot be made. If one assumes $n = 3$, the indexing can be made almost satisfactorily for all the observed reflections.

Natural minerals are known which show a similar X-ray diffraction pattern, manasseite ($a_0 = 3.06$ Å, $c_0 = 2 \times 7.67$ Å) and hydrotalcite ($a_0 = 3.06$ Å, $c_0 = 3 \times 7.67$ Å), whose compositions are $Mg_6Al_2(OH)_{16} \cdot CO_3 \cdot 4H_2O$, resp. The difference between their structures is caused only by the difference in the stacking of the unit layers. The structures of samples A–K are considered to be a repeated pile of the ABCABC type (rhombohedral system), in which a repeated pile of the ABAB type (hexagonal system) is partly included. A structral analysis of pyroaurite, $Mg_6Fe_2(OH)_{16}CO_3 \cdot 4H_2O$, of the hydrotalcite type, was made by Allmann *et al.* (1968).

Table 4. The cell dimensions (a_0, c_0) for samples A, G, J and K

Sample No.	Cell dimensions (Å) a_0	c_0 (Rhombohedral) $n = 3$	c_0 (Hexagonal) $n = 2$
A	3.06 Å	25.02 Å	16.68 Å
G	3.06	27.45	18.30
J	3.04	23.73	15.82
K	3.09	23.50	15.67

The relation of the Miller index to the reflection intensity and the symmetry for all samples, (003), (006), (110), and (113) is sharp and symmetric while (102), (105), and (108) is broad and asymmetric.

The integral breadth of the (006) plane is given in Table 5. Because the integral breadth of synthesized hydrotalcite is 0.67° at the atomic ratio of $Mg^{2+}:Al^{3+} = 3$ and the crystallite size is estimated to be 146 Å according to Sherrer's equation, the crystallite size should decrease in the order of Zn–Al–Cl Mg–Al–Cl Mg–Al–ClO_4 Mg–Al–NO_3 Ni–Al–Cl.

A comparison of sample D with F of the same composition reveals that the use of ammonia in the preparation of the compounds gives a better result. For the samples B–E with the same anion and different ratios of Mg^{2+}/Al^{3+}, a linear relation was obtained between the d_{003} and the ratios of $Mg^{2+}/(Mg^{2+} + Al^{3+})$ in the range of $0.6 < Mg^{2+}/(Mg^{2+} + Al^{3+}) < 0.9$, namely, Vergard's law holds. This indicates the substitution of Mg^{2+} in brucite layer by Al^{3+}.

Table 5. X-ray diffraction line broadening of (006) plane

Sample No.	The integral breadth of (006) reflection (degree)
A	2.17°2θ
B	1.20
C	0.76
D	0.86
E	0.58
F	0.37
G	1.24
H	1.40
I	0.85
J	1.86
K	0.37

https://doi.org/10.1346/CCMN.1975.0230508 Published online by Cambridge University Press

The lattice constant c_0 increases in the order of sample D > A > G and the anion size $Cl^- > NO_3^- > ClO_4^-$. In order to survey the relation in more detail, the thickness of the intermediate layer was calculated by subtracting the thickness (4.769 Å) of the brucite layer (Nihonkagakukai, 1966) from the thickness (d_{003}) of the unit layer. The calculated values, which are 3.36, 3.57 and 4.38 Å for D, A, and G, respectively, agree with the respective anion diameters, 3.62, 3.78 and 4.72 Å (Wyckoff, 1963).

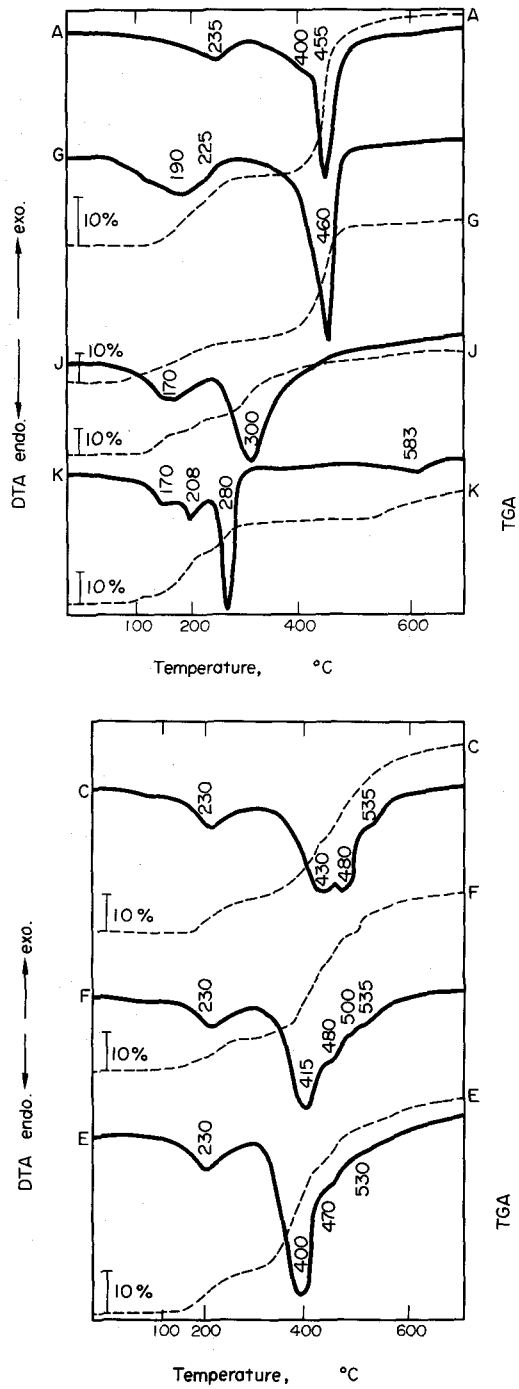

Fig. 2. (a) D.T.A. and T.G.A. curves for samples A, G, J and K. (b) D.T.A. and T.G.A. curves for samples C, F and E.

Thermal analysis

The DTA and TGA diagrams are shown in Fig. 2. Two peaks of heat absorption were observed around 200 and 300–500°C for every sample, the corresponding two stages of weight decrease being also observed (Rouxhet and Taylor, 1959). In order to examine the first peak of heat absorption, sample 1 was heat-treated in air at 200, 300 and 400°C for 1 hr and coated with polystyrene to protect moisture from entering (Miyata *et al.*, 1971) and then its X-ray diffraction pattern was observed. The similar pattern to that of the untreated sample, the pattern whose diffraction intensity was weakened with a little change of d, and the almost amorphous pattern were observed for the samples heat-treated at 200, 300 and 400°C, respectively. The samples heat-treated at 200 and 300°C which were allowed to stand in air for 48 hr without coating with polystyrene showed the same pattern as that of the untreated samples. These results indicate that the first heat absorption is due to the loss of interlayer water molecules as in the case of hydrotalcite and the second is due to the dehydroxylation and the elimination of anions giving rise to the destruction of the layer structurs.

The amount of interlayer water was determined by subtracting the weight loss of the sample when dried at 105°C for 3 hr, which is regarded as the amount of adsorbed water, from the first weight decrease on the TGA curve. The amount of OH^- was obtained by subtracting the first weight decrease and the amount of the ignition weight loss. The contents of NO_3^-, Cl^-, and ClO_4^- were calculated from the formulae of $2NO_3$–O, 2Cl–O, and $2ClO_4$–O, respectively, which correspond to the amount of each anion loss when the compounds were decomposed. Table 6 shows the chemical composition and charge. The reason why carbonate ions are contained in the samples is partly due to the insufficient decarbonation of aqueous solution of sodium hydroxide. The reason that the total number of cations ranges from 6 to 10 is due to the fact that hydrotalcite-like compounds, in which Mg^{2+} is substituted by Al^{3+}, with the ratio of $Mg^{2+}/Al^{3+} \fallingdotseq 2$–10 are formed (Miyata *et al.*, 1971). The ratio of the positive charge of the basic layer to that of the aluminimum ion is almost unity for all samples except sample K. Thus, the positive charge of the basic layer is determined by the amount of substituted aluminum ion. Because the negative charge of the intermediate layer is almost equal to the positive charge of the basic layer, the anions act to neutralize the positive charge. The existence of the interlayer water is due to the positive charge of the basic layer and, therefore, ammonia, etc. other than water are also able to enter the interlayer.

For the compounds of Zn^{2+}, besides $Zn(OH)_2$ of coordination number = 4, these are β-Zn(OH)Cl (Wyckoff, 1973) and $Zn_5(OH)_8Cl_2$ (A.S.T.M., 1967) of

https://doi.org/10.1346/CCMN.1975.0230508 Published online by Cambridge University Press

Table 6. Chemical composition and charge

Sample	Basic layer	Interlayer
A composition	$[Mg_{5.74}Al_2(OH)_{15.40}]$	$[(NO_3)_{1.66}(CO_3)_{0.13}\ 2.15\ H_2O]$
charge	+2.08	−1.92
C composition	$[Mg_{4.09}Al_2(OH)_{12.21}]$	$[Cl_{1.61}(CO_3)_{0.15}\ 1.17\ H_2O]$
charge	+1.97	−1.91
E composition	$[Mg_{7.72}Al_2(OH)_{19.39}]$	$[Cl_{1.93}(CO_3)_{0.12}\ 2.73\ H_2O]$
charge	+2.05	−2.17
F composition	$[Mg_{6.00}Al_2(OH)_{15.75}]$	$[Cl_{1.81}(CO_3)_{0.15}\ 2.10\ H_2O]$
charge	+2.25	−2.11
G composition	$[Mg_{6.12}Al_2(OH)_{16.23}]$	$[(ClO_4)_{1.46}(CO_3)_{0.15}\ 3.72\ H_2O]$
charge	+2.01	−1.76
J composition	$[Ni_{5.75}Al_2(OH)_{15.40}]$	$[Cl_{1.73}(CO_3)_{0.23}\ 1.99\ H_2O]$
charge	+2.10	−2.19
K composition	$[Zn_{6.08}Al_2(OH)_{15.50}]$	$[Cl_{2.39}(CO_3)_{0.19}\ 2.18\ H_2O]$
charge	+2.65	−2.77
K′ composition	$[Zn_{6.08}Al_2(OH)_{15.50}Cl_{0.71}]$	$[Cl_{1.68}(CO_3)_{0.19}\ 2.18\ H_2O]$
charge	+1.94	−1.94

coordination number = 6. From this fact and the result of DTA described below, it seems more valid to rewrite the composition of sample K to K′ in Table 6.

Because there is a space corresponding to the oxygen ions whose number is the same as the sum of M^{2+} and M^{3+}, the amount of interlayer water can be determined by subtracting the space occupied by an anion of the intermediate layer from the space of the oxygen ion (Allmann, 1970). Assuming that the size of NO_3^-, CO_3^{2-} or Cl^- corresponds to that of 3 oxygen ions, the amount of the interlayer water is calculated to be $6.00 + 2.00 - (0.15 \times 3 + 1.81 \times 3) = 2.12$ for sample F of a comparatively large crystal. The calculated values for other samples are shown in Table 7. For sample A, if the size of NO_3^- is approx. that of three oxygens, the result supports the validity of the assumption. The calculated values for samples E, F, and J containing Cl^- are almost equal to the observed values. However, it is noted that the ratio of the observed value to the calculated one becomes large with an increase of substituted Al^{3+}. In particular, the observed value is apparently larger than the calculated one for sample C. This is probably caused by the increase in positive charge on the basic layer with increasing substituted Al^{3+}. In sample G, the observed value was about two times as large as the calculated one. This is probably due to the existence of water of a bimolecular layer, since d_{003} is about 1.8 Å larger compared to sample F and the first heat absorption in the DTA curve is divided into two peaks at 190 and 225°C. In sample K, the observed value was about 6 times larger than the calculated one. However, the result is valid for the composition of sample K′. From the above argument, it can be said that the calculated values are in fairly good agreement with the observed ones.

Table 7. Calculation of interlayer water content

Sample	Interlayer water content (H_2O/Al_2O_3)	
A	2.37	(molar ratio)
C	0.81	
E	3.11	
F	2.16	
G	1.87	
J	1.87	
K	0.34	
K′	2.47	

The DTA curve observed for sample A was similar to that for hydrotalcite, since the structure of NO_3^- is the same as that of CO_3^{2-}. For the samples other than G, the first peak areas were smaller than that of hydrotalcite. Two peaks at 190 and 225°C observed for sample G indicate the existence of two kinds of interlayer water as mentioned before. The decomposition temperature of $Ni(OH)_2$ is 230°C (Kagakudaiziten, 1967), but that of sample J is 300°C as shown in Fig. 2(a), indicating that the latter is the more stable. The desorption temperature of interlayer water in sample J as well as sample K was lower than that of other samples. In the case of sample K, the peak at 170°C is thought to be due to the desorption of the interlayer water. On the analogy of the results for samples C, E and F as described below, the peaks at 208, 280 and 583°C are considered to be due to the eliminations of OH^- and Cl^- in the basic layer and Cl^- in the intermediate layer, respectively. The fact that the decomposition temperature of $Zn(OH)_2$ is 125°C (Kagakudaiziten, 1967) and OH^- in the basic layer of sample K is more stabilized supports the above view.

In the case of samples C,E,F which have different ratios of Mg^{2+}:Al^{3+}, the second heat absorption peak is split into three or four peaks. The first peak of the second heat absorption shifts gradually to higher temperature (400–430°C) with a decrease of the ratio of Mg^{2+}:Al^{3+} and the ratio of the area of the other peaks (470–480°C) to the area of the first peak decreases in the order of sample C > F > E. This corresponds to a tendency of the increase in the ratio of Cl^-:OH^-. The amount of Cl^- was found to decrease rapidly when sample F was heat-treated in air above 450°C for 1 hr. Hence, the first and the other

https://doi.org/10.1346/CCMN.1975.0230508 Published online by Cambridge University Press

peaks of the second heat absorption are considered to be caused by the elimination of OH^- in the basic layer and Cl^-, respectively.

I.r. absorption spectra

The i.r. spectra of sample A in the range of 400–1800 cm^{-1} are shown in Fig. 3. The assignment of the absorption bands of NO_3^- was made by referring to the study on the complex, $Ni(en)_2(NO_3)_2$ (Curtis and Curtis, 1966). Since a weak ν_1 vibration (1050 cm^{-1}) appears and ν_2 and ν_3 vibrations are split into two (820, 840 cm^{-1}) and four peaks (1230, 1370–1390, 1480–1500, and 1680–1705 cm^{-1}), NO_3^- is coordinated as mono- or bidentate. In the case of hydrotalcite ($Mg^{2+}/Al^{3+} = 3$) heat-treated in air above 400°C for 2 hr, two split peaks due to ν_3 vibration appear at 1235 and 1700 cm^{-1}, besides the two split peaks (1380 and 1530 cm^{-1}) of ν_3 which are observed for the hydrotalcite heat-treated below 300°C. Hence, the four peaks due to ν_3 are consist of two pair of peaks (a pair of 1370–1390 cm^{-1} and 1480–1500 cm^{-1} and another of 1230 cm^{-1} and 1680–1705 cm^{-1}). The width of splitting of each pair is about 110 and 460 cm^{-1}, respectively and the absorption intensity of the latter is much weaker than that of the former. Therefore, a small part of NO_3^- is coordinated as bidentate but most of it is monodentate.

The i.r. spectrum of sample G in the range of 400–1300 cm^{-1} and the band assignment are shown in Fig. 3. Since ν_1 and ν_2 appear at 943 and 476 cm^{-1} and ν_3 and ν_4 are split into four peaks (1150, 1126, 1112, and 1095 cm^{-1}) and two or three peaks (640, 629–633 cm^{-1}) respectively, ClO_4^- is considered to exist as a bidentate complex (Nakamoto, 1970). There are two kinds of bidentate; chelate and bridge type. The difference can be determined by the width of ν_3 splitting (Nakamoto, 1970). For example ν_3 is split into 210 and 50 cm^{-1} in the case of $[Cu(biph)SO_4]$ $2H_2O$ and into 4 peaks for bridge type. The ν_3 of mono- and bidentate ClO_4^- are split into 23–28 cm^{-1} and 72–323 cm^{-1} and the ν_4 appears at 912–920 and 920–1030 cm^{-1} respectively. Therefore, since the width of ν_3 splitting is 55 cm^{-1} and ν_4 appears at 940 cm^{-1} for sample G, the ClO_4^- in the sample is coordinated as bidentate of bridge type.

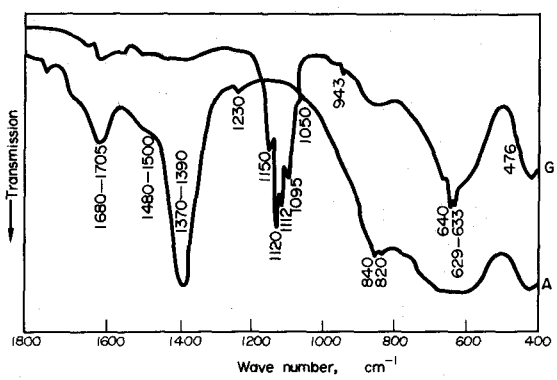

Fig. 3. I.r. absorption spectra in the region of 400–1800 cm^{-1} for samples A and G.

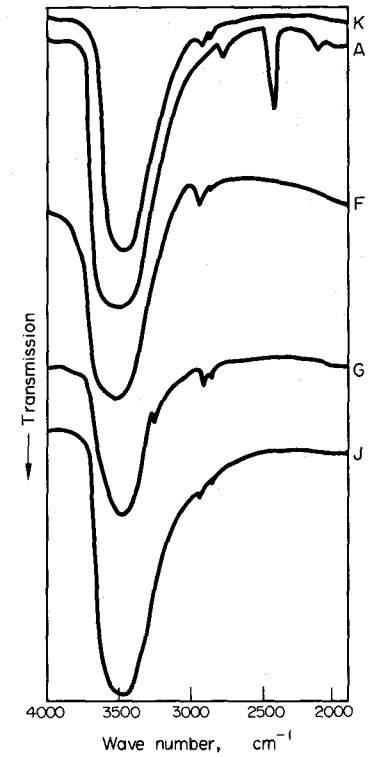

Fig. 4. I.r. absorption spectra in the region 1600–4000 cm^{-1} for samples A, F, G, J and K.

The i.r. spectra of various samples in the range of 1600–4000 cm^{-1} are shown in Fig. 4. In all samples, a strong absorption band was observed at 3465–3510 cm^{-1}, but no band of isolated OH^- was found, indicating that all OH^- are hydrogen-bonding. The distance of oxygen–oxygen bond corresponding to each vibration (Lippincott and Schroeder, 1955) is about 2.85–2.95 Å, which seems to be the hydrogen bond distance between OH^- in the basic layer and H_2O or anion in the intermediate layer. The shoulder at 3100–3200 cm^{-1} is due to the hydrogen bond between H_2O and the anion in the intermediate layer, the distance corresponding to the vibration being about 2.7–2.75 Å.

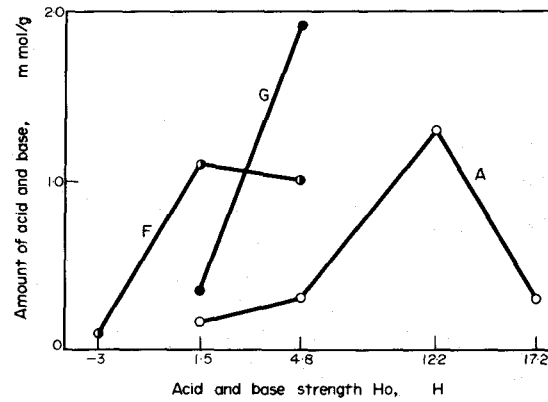

Fig. 5. Acidity and basicity for samples A, F and G (calcination temp. 500°C).

https://doi.org/10.1346/CCMN.1975.0230508 Published online by Cambridge University Press

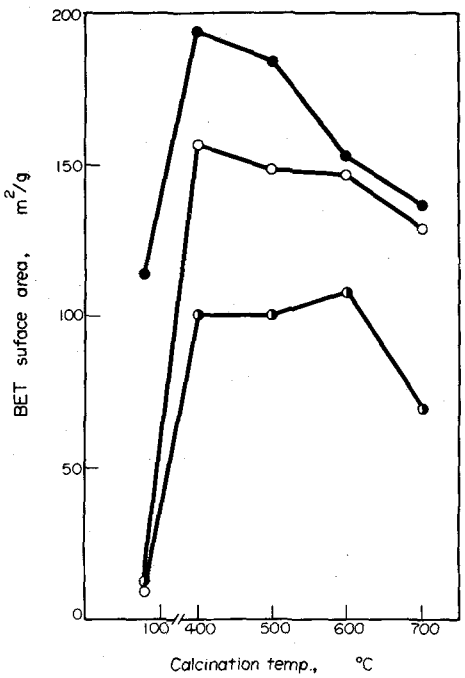

Fig. 6. BET surface area at different calcination temperature for samples A, F and G.

Acidic and basic property

Figure 5 shows the acidic and basic property of samples A, F, and G calcined in air at 500°C for 1 hr. Sample A showed this property to be similar to hydrotalcite. The fact that samples F or G containing Cl^- or ClO_4^- did not show any basic property is probably caused by the poisoning of the basic sites with Cl^- or ClO_4^- which is more acidic than NO_3^- or CO_3^{2-}.

Specific surface area

Figure 6 shows the specific surface area of samples A, F and G calcined in air at 400–700°C for 1 hr. The surface area of sample A and its change with calcination temperature were almost the same as those of synthesized hydrotalcite. The maximum value was observed at the temperature of structure destruction without much sintering at 400–600°C. The crystal phase in the temperature range is only MgO, and $MgAl_2O_4$ is newly formed at about 900°C, according to X-ray diffraction. Therefore, the substituted Al^{3+} is considered to control the growth of the MgO crystal.

Structural model of new hydrotalcite-like compounds

On the basis of these results and discussion, the structure is considered to consist of a positively charged basic layer $[M_x^{2+}M_y^{3+}(OH)_{2(x+y)}]^{y+}$ and an intermediate layer of anions and water molecules, shown schematically in Fig. 7. The hydroxyl group of the basic layer is hydrogen-bonded with water or anion of the intermediate layer and the interlayer water is hydrogen-bonded with the interlayer anion.

REFERENCES

Allmann, R. (1968) The crystal structure of pyroaurite: *Acta Cryst.* **24,** 972.

Allmann, K, (1970) Doppelschichtstrukturen mit brucitähnlichen schichtionen: *Chemia* **24,** 99.

A.S.T.M. (1967) Powder diffraction file, Inorg., A.S.T.M., Philadelphia, U.S.A., **226,** 530.

Brown, G. and Gastuche, M. C. (1967) Structure and structural chemistry of synthetic hydroxycarbonates and related minerals and compounds—II: *Clay Minerals* **7,** 193.

Curtis N. F. and Curtis Y. M. (1966) Some nitrate–amine nickel(II) compounds with monodentate and bidentate nitrate ions: *Inorg. Chem.* **5,** 383.

Kagakudaiziten Editorial Committee (1967) *Kagakudaiziten* **5,** Kyoritsu, Tokyo, Japan, 18 33.

Kobo, B., Miyata, S., Kumura, T., and Shimada, T. (1969) Physical and chemical characteristics and antacid activities of synthetic hydrotalcite: *Yakuzaigaku* **29,** 215.

Lippincott, E. R. and Schroeder, R. (1955) One-dimensional model of the hydrogen bond: *J. Chem. Phys.* **23,** 1099.

Miyata, S. and Kumura, T. (1973) Syntheses of new hydrotalcite-like compounds and their physico–chemical properties: *Chem. Lett.* p. 843.

Miyata, S., Kumura, T., Hattori, H. and Tanabe, K. (1971) Physico–chemical properties and structure of magnesia–alumina: *Nippon Kagaku Zasshi* **92,** 514.

Nakamoto, K. (1970) *I.r. Spectra Inorganic and Coordination Compounds.* Wiley, New York, pp. 171, 175, 176.

Nipponkagakukai (1966) *Kagakubinran, Kisohen,* **2,** Maruzen, Tokyo, Japan 1265.

Rouxhet, P. C. and Taylor, H. F. W. (1959) Thermal decomposition of sjögrenite and pyroaurite: *Chemia* **23,** 480.

Wyckoff, R. W. G. (1963) *Crystal Structure,* Vol. 1. Wiley, New York, p. 282.